Catalysis Science & Technology

Accepted Manuscript

ROYAL SOCIETY OF CHEMISTRY

www.rsc.org/catalysis

Non-mercury catalytic acetylene hydrochlorination over activated carbon-supported Au catalysts promoted by CeO_2

Guangbi Li,[a,b] Wei Li[a], and Jinli Zhang*[a]

[a] School of Chemical Engineering and Technology, Tianjin University, Tianjin 300072, P. R. China

[b] College of Chemical Engineering and Materials Science, Tianjin University of Science and Technology, Tianjin 300457, P. R. China

*Corresponding Author: Dr. Jinli Zhang
Professor of Chemical Engineering
School of Chemical Engineering and Technology
Tianjin University, Tianjin 300072, P. R. China
Tel: +86-22-27890643
Fax: +86-22-27890643
E-mail: zhangjinli@tju.edu.cn

Abstract

Gold-cerium oxide catalysts were prepared to study the effects of cerium oxide additives on the catalytic performance of gold catalysts for acetylene hydrochlorination, using activated carbon as the support. The optimal catalytic performance is achieved over 1Au–5CeO_2/AC catalyst with the acetylene conversion of 98.4% and the selectivity to vinyl chloride monomer (VCM) of 99.9% after 20 h on stream under the conditions of 180 °C, C_2H_2 gas hourly space velocity (GHSV) of 852 h^{-1}, and the feed volume ratio HCl/C_2H_2 of 1.15. It is indicated that the addition of cerium oxide can make active Au species dispersed uniformly and improve the adsorption property of reactants on the catalysts, but also suppress the reduction of active gold species and inhibit the coking deposition on the catalyst surfaces during the reaction, characterized with transmission electron microscopy, Raman spectroscopy, N_2 adsorption/desorption analysis, thermogravimetric analysis, temperature-programmed reduction, temperature-programmed desorption, powder X-ray diffraction, atomic absorption spectrophotometer and X-ray photoelectron spectroscopy.

Keywords: Au-based catalysts; cerium oxide; acetylene hydrochlorination; heterogeneous catalysis

1. Introduction

Acetylene hydrochlorination is one of significant industrial processes to produce

vinyl chloride monomer (VCM) for polyvinyl chloride (PVC) industry, particularly in countries enriched with coal.[1,2] However, the current mercuric chloride industrial catalyst for acetylene hydrochlorination reaction will be prohibited by the United Nations in the near future,[3,4] due to high toxicity and serious environmental pollution of mercuric chloride. Therefore, it is urgent to develop an efficient non-mercury catalyst with high activity and long stability for acetylene hydrochlorination.

Since the pioneer work of Hutchings,[5] the activated carbon-supported gold catalysts (Au/AC) have been studied as the promising non-mercury catalyst for acetylene hydrochlorination[6–9]. Although the initial rate over Au catalysts is higher than other metal chloride including mercury chloride, the deactivation rate of Au catalysts is much faster, which is attributed to the reduction of Au^{3+} active species and the coking deposition during the reaction.[8,10] In recent years, many works have been reported on metal additives to improve the catalytic performance of Au catalysts for acetylene hydrochlorination.[7,9,11–17] For examples, Huang et al.[16] studied the effect of TiO_2 additive on the catalyst performance of Au catalysts, and concluded that the acetylene conversion of the optimal $10TiO_2$–$AuCl_3$/AC catalyst decreased from 92% to 81% after 10 reaction under reaction conditions of 180 °C, V_{HCl}/V_{C2H2} ratio of 1.15, and GHSV (C_2H_2) of 870 h^{-1}. Zhang et al.[18] synthesized the ternary Au–Co(III)–Cu(II) catalysts and found that over the optimal catalyst Au1Co(III)3Cu(II)1/SAC the acetylene conversion reached 99.7% and the selectivity to VCM is 99.9% within 48 h under the reaction conditions of 150 °C, V_{HCl}/V_{C2H2} ratio of 1.15, and GHSV (C_2H_2) of 360 h^{-1}. However, it is still a challenge to modify the catalytic performance of

Au-based catalysts in order to achieve an efficient and long-term stable non-mercury catalyst for acetylene hydrochlorination in the view of PVC manufacture industry.

Au–CeO_2 catalyst have been widely studied in the reactions of CO oxidation,[19–22] water–gas shift (WGS),[23,24] and formaldehyde oxidation,[25] owing to the strong interactions between Au species and ceria.[19,26] We are enlightened to study whether or not the CeO_2 additive can improve the catalytic performance of Au-based catalysts for acetylene hydrochlorination. In this paper, we prepared a series of activated carbon-supported Au–CeO_2 catalysts through the immersion method and studied the catalytic performance for acetylene hydrochlorination, in combination with characterizations of TEM, XRD, Raman, XPS, etc.

2. Experimental

2.1 Materials

$HAuCl_4 \cdot 4H_2O$ (Au assay ≥ 47.8%) and CeO_2 (assay ≥ 99.9%) were purchased from Sinopharm Chemical Reagent Co., Ltd, China; Activated carbon (AC, neutral, coconut carbon, 20–40 mesh) was supplied by SenSen Activated Carbon Industry Science and Technology Co., Ltd., Fujian, China. All the other materials and chemicals were commercially available and used without any purification.

2.2 Catalyst preparation

Au–CeO_2/AC catalysts were prepared using the impregnation technique with aqua regia as a solvent.[7,16] About 44.79 mg of CeO_2 was dissolved in 7.50 mL aqua regia,

stirring at room temperature (RT) for 30 min, and then 5 g AC was added to the mixture under stirring. After drying for 24 h at RT, about 5.36 mL (solution, 1 g of $HAuCl_4$ was dissolved in 50 mL aqua regia) $HAuCl_4$ aqua regia solution was added, and the mixture was maintained under stirring for 24 h, evaporated in steam bath, then dried at 150 °C for 14 h and used as a catalyst. The obtained catalyst with a Ce/Au molar ratio of 1:1 was denoted as 1Au–1CeO_2/AC. Similarly, other catalysts 1Au–3CeO_2/AC, 1Au–5CeO_2/AC, and 1Au–10CeO_2/AC were prepared via the above procedure with the Ce/Au molar ratio of 3:1, 5:1, and 10:1, respectively. As a control, Au/AC and 1CeO_2/AC (the metallic content is 1.0 wt. %) were also prepared in the similar procedure. The loading content of Au in all these catalysts was fixed as 1.0 wt. %.

2.3 Catalytic performance evaluation

The catalytic performance of the catalyst sample was investigated using a fixed-bed glass microreactor (i.d. of 8 mm). The temperature of the microreactor was regulated by a CKW–1100 temperature controller produced by Chaoyang Automation Instrument Factory, Beijing, China. Acetylene (99.9 % purity) was passed through silica-gel desiccant to remove trace impurities, and hydrogen chloride gas (99.9 % purity) was dried using 5A molecular sieves. Acetylene (14.2 mL min^{-1}) and hydrogen chloride (16.3 mL min^{-1}), calibrated by mass flow controllers to provide the C_2H_2 gas hourly space velocity (GHSV) of 852 h^{-1}, were introduced into a heated reactor containing catalyst (1 mL) operated under the pressure of 1.1~ 1.2 bar at

180 °C. The reactor effluent was passed through an absorption bottle containing sodium hydroxide solution to remove unreacted hydrogen chloride. And then, the gas mixture was analyzed by Beifen GC–3420A gas chromatograph (GC).

2.4 Catalyst characterization

Low-temperature N_2 adsorption/desorption experiments were conducted using a Micromeritics ASAP 2020C surface area analyzer. The samples were first degassed at 150 °C for 6 h and analyzed via liquid nitrogen adsorption at –196 °C.

Thermogravimetric analysis (TGA) of the samples was conducted using a TA Instruments SDT Q600 under air atmosphere at a flow rate of 100 mL min^{-1}. The temperature was increased from 35 to 900 °C at a heating rate of 10 °C min^{-1}.

Powder X-ray diffraction (XRD) measurements were performed on a Bruker D8 Focus diffractometer using Cu Kα radiation with 4° min^{-1} scan speed and 20–80° scan range at 40 kV and 40 mA.

H_2 temperature-programmed reduction (TPR) and He temperature-programmed desorption (TPD) experiments were performed using a Micromeritics AutoChem II 2920 analyzer equipped with a thermal conductivity detector (TCD). The weight of the tested samples was 50 mg and 100 mg respectively for TPR and TPD experiments. Prior to each test, the samples were treated with N_2 gas at 100 °C for 1 h. After cooling, the temperature was increased from 50 to 800 °C at a heating rate of 10 °C min^{-1} with a 10.0 % H_2/Ar atmosphere flowing at a rate of 20 mL min^{-1} for TPR and a He atmosphere for TPD experiments.

Transmission electron microscopy (TEM), High-resolution TEM and energy dispersive X-ray spectrometer (EDS) were performed on a JEM–2100F field emission transmission electron microscope (JEOL, Tokyo, Japan) working at 200 kV using a scanning TEM mode. For sample preparation, the samples were ground in an agate mortar and ultrasonically dispersed in ethanol, and a drop was then deposited on a carbon-coated copper grid and dried. The sizes of Au nanoparticles on the samples were observed by TEM images and determined from a count of 200 particles.

X-ray photoelectron spectra (XPS) were obtained using a PHI 5000 Versaprobe (ULVAC–PHI Inc., Osaka, Japan) employing monochromatic Al Kα X-rays (hν = 1486.7 eV) under high vacuum condition. The data were collected at a sample tilt angle of 45°. The binding energies were corrected using the C 1s peak of aliphatic carbon at 284.8 eV as an internal standard.

The gold content in all samples was determined using an air–acetylene flame atomic absorption spectrophotometer (Perkin–Elmer, AAS 800) according to the recommended conditions.

Raman spectra were measured using a DXR Raman Microscope (DXR Microscope, ThermoFisher, USA) with a 532 nm argon ion laser as the excitation source at room temperature.

3. Results and discussion

3.1 Catalytic performance for acetylene hydrochlorination

Three kinds of catalysts, involving 1Au–1CeO_2/AC, Au/AC and 1CeO_2/AC, were

evaluated for acetylene hydrochlorination, together with the blank support AC, in order to study the effect of CeO_2 additive on the performance of Au-based catalyst. As shown in Fig. 1, the acetylene conversion is respectively 5.2% over the blank support, 4.6% over $1CeO_2$/AC, 72.5% over Au/AC, and 94.8% over $1Au–1CeO_2$/AC at 10 h, but it decreases respectively to 4.6%, 4.2%, 55.0%, and 88.7% after 20 h reaction. The results show that AC and $1CeO_2$/AC display very poor catalytic activity for acetylene hydrochlorination reaction. The selectivity to VCM over all these catalysts and support AC is greater than 98.4% (Fig. 1b). It is clear that the CeO_2 additive can enhance the catalytic activity and the stability of Au-based catalysts for acetylene hydrochlorination.

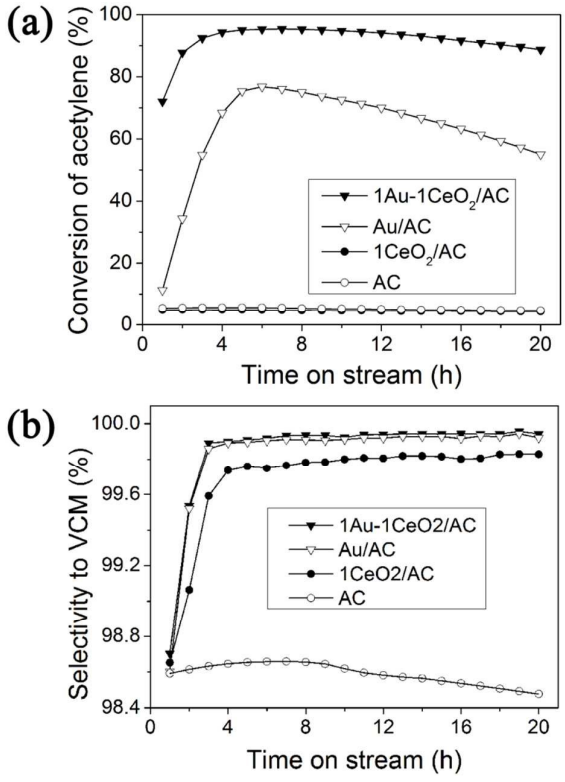

Fig. 1 The catalytic performance of different catalysts for acetylene hydrochlorination.

Conditions: temperature = 180 °C; GHSV (C_2H_2) = 852 h^{-1}; feed volume ratio V_{HCl}/V_{C2H2} = 1.15.

The effect of the Ce/Au molar ratio was studied on the performance of Au-based catalysts for acetylene hydrochlorination. As shown in Fig. 2a, over the catalysts 1Au–xCeO_2/AC (x = 1, 3, 5, or 10), the acetylene conversion is respectively 94.8%, 95.9%, 99.1% and 98.1% at 10 h, whereas it decreases respectively to 88.7%, 91.5%, 98.4% and 96.5% after 20 h. Over these catalysts with the molar ratio of Ce/Au ranged from 1 to 10, the selectivity to VCM is greater than 99.0% (Fig. 2b). It is remarkable that the catalyst 1Au–5CeO_2/AC exhibits the optimal catalytic performance for acetylene hydrochlorination, with the acetylene conversion higher than the values in previous literature about Au-based catalysts[6,7,16,27]. However, with much higher content of CeO_2, the catalyst 1Au–10CeO_2/AC shows a little lower acetylene conversion than 1Au–5CeO_2/AC. It is indicated that the excessive CeO_2 additive may tend to block the pore and decrease the active surface area, resulting in a decrease of catalytic activity.

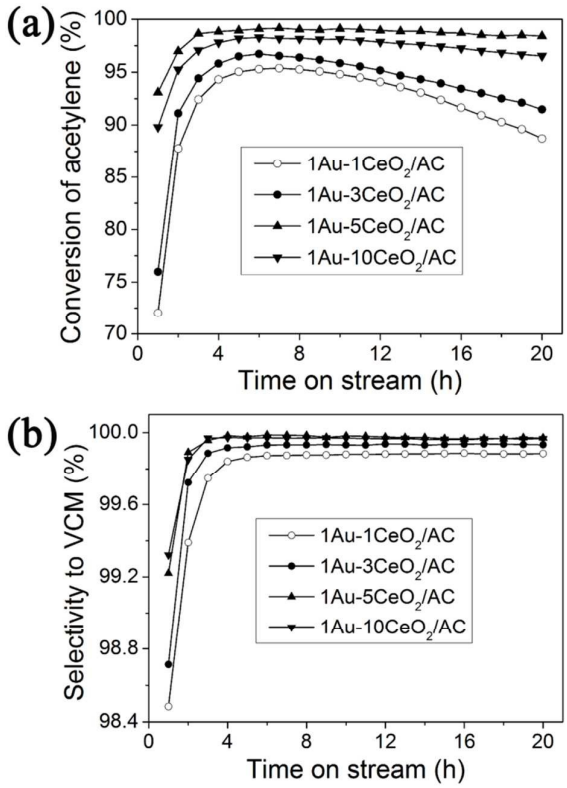

Fig. 2 Effect of CeO_2 additive on the catalytic performance of the Au-based catalysts. Conditions: temperature = 180 °C; GHSV (C_2H_2) = 852 h^{-1}; feed volume ratio V_{HCl}/V_{C2H2} = 1.15.

3.2 Catalyst characterization

Au–CeO_2 catalysts were characterized by BET, TGA, TPR, TPD, Raman, XRD, TEM, and XPS, etc., to study effects of CeO_2 additive on the structure and physicochemical properties of gold catalysts.

3.2.1 TEM images and Raman spectra studies

Fig. 3 displays the typical TEM images and particle size distribution, HRTEM image, EDS and Raman spectra of Au-based catalysts. As shown in Fig. 3a and 3c, the average particle size of the fresh catalyst Au/AC is about 2.95 nm, determined from a

count of 200 particles in TEM images. While for the fresh catalyst 1Au–5CeO_2/AC, there are several large particles with the size about 28 nm, which are mainly composed of ceria (Fig. 3b). In these large particles there display abundant crystal lattices of 0.32 nm for the CeO_2 (111) together with a dispersed lattice of 0.23 nm for Au (111) (Fig. 3e).[25] EDS and Raman spectra indicate the existence of both CeO_2 and Au (Fig. 3d and 3f).

We have measured TEM and HRTEM images for a number of catalyst samples 1Au–5CeO_2/AC. There is one exception TEM image showing small gold particles, as shown in Fig. S1a, there are two large particles (about 25 nm) due to ceria, reflected by the crystal lattices of 0.32 nm for the CeO_2 (111) (Fig. S1d); while other small particles are gold nanoparticles with the crystal lattice of 0.23 nm for Au (111) (Fig. S1c). The gold nanoparticles have an average particle size about 1.67 nm (Fig. S1b). In combination with Fig. 3, it is suggested that the gold species are highly dispersed in the fresh catalyst 1Au–5CeO_2/AC.

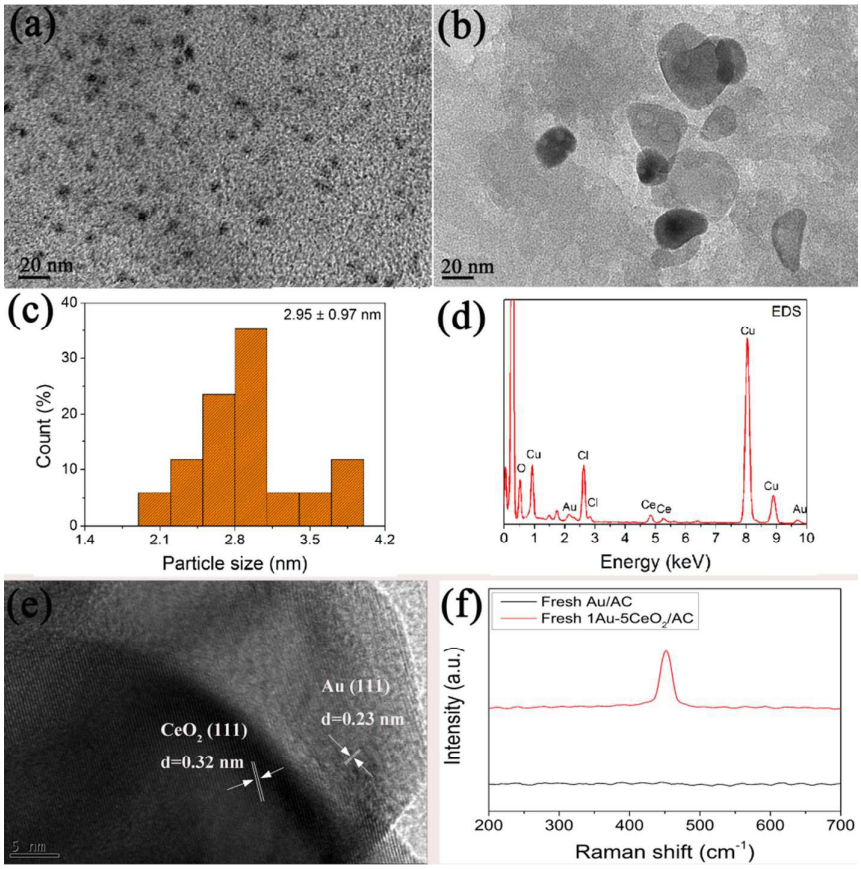

Fig. 3 TEM images of the fresh catalyst Au/AC (a), and the fresh catalyst 1Au–5CeO_2/AC (b); and the particle size distribution of the fresh catalyst Au/AC (c), and the EDS spectrum of the fresh catalyst 1Au–5CeO_2/AC (d), and the HRTEM image of the fresh catalyst 1Au–5CeO_2/AC (e), and Raman spectra of the fresh catalysts Au/AC and 1Au–5CeO_2/AC (f).

3.2.2 Effect of CeO_2 additive on the texture property and carbon deposition of Au-based catalysts

Low temperature N_2 adsorption/desorption experiments were performed to evaluate the texture properties of Au-based catalysts with the addition of CeO_2. As listed in Table 1, the specific surface area and total pore volumes of Au-based catalysts

decrease after loading the active gold species on AC or adding CeO_2 additive to Au/AC, probably due to the block of pores by active gold species or the CeO_2 additive. In addition, the specific surface area and total pore volumes of the used catalysts are lower than those of the fresh catalysts. After 20 h reaction, the BET specific surface area and total pore volumes of the used Au/AC are decreased by 24.9% and 25.0%, respectively. The addition of CeO_2 reduces the variation of specific surface area (ΔS_{BET}%) before and after reaction, following the order: 1Au–1CeO_2/AC (16.0%) > 1Au–3CeO_2/AC (13.4%) > 1Au–10CeO_2/AC (11.1%) > 1Au–5CeO_2/AC (9.8%), so does the variation of total pore volumes. According to measurements by AAS, the used catalysts show no obvious variation of Au loading content (Table S1). It is suggested that the decrease of catalytic activity (Fig. 2) is caused partially by the loss of specific surface area of Au-CeO_2/AC, in particular, with the Ce/Au molar ratio of 5, the reduce extent of the specific surface area is the least, consequently corresponding to the highest activity over 1Au–5CeO_2/AC.

Table 1 Pore structure parameters of the catalysts.

Catalyst	S_{BET} (m^2 g^{-1})		Total pore volume(cm^3 g^{-1})	
	Fresh	Used	Fresh	Used
AC	1126	/	0.639	/
Au/AC	1047	786	0.588	0.441
1Au–1CeO_2/AC	993	834	0.558	0.469
1Au–3CeO_2/AC	967	837	0.543	0.470
1Au–5CeO_2/AC	950	857	0.533	0.481
1Au–10CeO_2/AC	932	829	0.523	0.465

Thermogravimetric analysis (TGA) was carried out to measure the amount of coking deposition over the catalysts 1Au–xCeO_2/AC (x = 0, 1, 3, 5, or 10) after 20 h reaction. Fig. S2a displays the typical TGA curves of the fresh and used Au/AC, neither the fresh nor the used Au/AC has obvious weight loss before 150 °C, indicating small amount of water adsorbed on the catalyst surface. The fresh catalyst Au/AC displays a weight loss about 8.43% in the range of 150 ~ 450 °C. When the temperature is above 450 °C, the fast weight loss is caused by the combustion of activated carbon.[28] In comparison, the used Au/AC catalyst has a larger weight loss (12.03%) in the range of 150 ~ 450 °C, mainly due to the combustion of coking deposition on the catalyst surface. Therefore, the actual amount of coking deposition on the used catalyst Au/AC is 3.60%, which is calculated by a previous reported method.[29]

Upon the addition of CeO_2 with the optimal Ce/Au molar ratio of 5, TGA curves of the fresh and used catalyst 1Au–5CeO_2/AC show respectively the weight loss of 8.37% and 9.46% in the range of 150 ~ 450 °C (Fig. S2b). Similarly the coking deposition on the used catalyst 1Au–5CeO_2/AC is calculated as 1.09%, which is the lowest in Table 2. It is clear that the amount of coking deposited on the used Au/AC is the highest, following the order of Au/AC (3.60%) > 1CeO_2/AC (2.82%) > 1Au–1CeO_2/AC (2.43%) > AC (1.88%) > 1Au–3CeO_2/AC (1.76%) > 1Au–10CeO_2/AC (1.67%) > 1Au–5CeO_2/AC (1.09%). The results suggest that the amount of coking deposition is reduced greatly by the CeO_2 additive over the Au–CeO_2/AC catalysts. It is worthy to note that the amount of coking deposition on the used catalyst 1Au–

10CeO_2/AC is higher than that on 1Au–5CeO_2/AC, suggesting that the excessive CeO_2 additive results in more coking deposition on the catalyst surface and then reducing the catalytic activity, in accord with the activity results in Fig. 2.

Table 2 Carbon deposition on the used catalysts.

Catalyst	Amount of carbon deposition (%)
AC	1.88
1CeO_2/AC	2.82
Au/AC	3.60
1Au–1CeO_2/AC	2.43
1Au–3CeO_2/AC	1.76
1Au–5CeO_2/AC	1.09
1Au–10CeO_2/AC	1.67

3.2.3 Effect of CeO_2 additive on the reducibility and adsorption property of gold catalyst.

H_2-TPR was used to evaluate the reducibility of the fresh catalysts 1Au–xCeO_2/AC (x = 0, 1, 3, 5, or 10). It is known that the surface of activated carbon consists of oxygenated groups[30] and heteroatoms[31]. The reduction bands of 1Au–xCeO_2/AC (x = 0, 1, 3, 5 or 10) in the range of 400 ~ 800 °C are associated with the interactions among gold species, CeO_2 and those functional groups on activated carbon surfaces.[32–34] As shown in Fig. 4, the fresh catalyst Au/AC exhibits a characteristic reduction peak in the range of 270 ~ 400 °C with the center at 362 °C, which is attributed to the reduction of Au^{3+} species.[13] With the increase of Ce/Au molar ratio,

the reduction temperature of Au^{3+} species decreases gradually. When the Ce/Au molar ratio is 5, the fresh catalyst 1Au–5CeO_2/AC shows the lowest reduction temperature of Au^{3+} species around 336 °C. The easy reducibility of Au^{3+} in the catalyst 1Au–5CeO_2/AC suggests that the addition of CeO_2 can make the Au species dispersed well, comparing with that of Au/AC. For the catalyst Au/AC, Fig. 3c shows that gold nanoparticles on the surface of activated carbon support have an average particle size about 2.95 nm. While for the catalyst 1Au–5CeO_2/AC, most of gold species are highly dispersed on the surface of the fresh catalyst 1Au–5CeO_2/AC, except of a few gold nanoparticles have an average particle size about 1.67 nm (Fig. 3b, 3d, 3e, and Fig. S1b). The high dispersion of gold species in the catalyst 1Au–5CeO_2/AC can provide more active sites to catalyze the acetylene hydrochlorination reaction, consequently resulting in high catalytic activity, consistent with the results in Fig. 2.

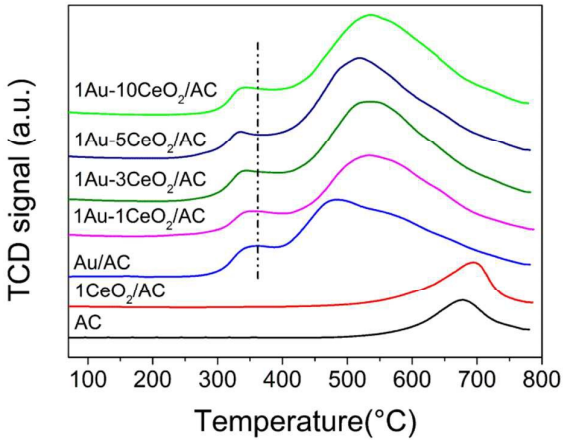

Fig. 4 H_2-TPR profiles of the fresh Au-CeO_2/AC catalysts.

TPD experiments were performed to examine the effect of CeO_2 additive on the

adsorption properties of reactants, acetylene and hydrogen chloride, over the fresh catalysts 1Au–xCeO_2/AC (x = 1, 3, 5, or 10). As shown in Fig. 5a, the fresh Au/AC exhibits two obvious desorption peak of acetylene in the range of 180 ~ 600 °C. While the catalysts 1Au–xCeO_2/AC (x = 1, 3, 5, or 10) exhibits a broad desorption peak of acetylene ranging from 250 ~ 600 °C, and the desorption areas of acetylene from the catalysts 1Au–xCeO_2/AC (x = 1, 3, 5, or 10) are obviously larger than that of the Au/AC. For another reactant hydrogen chloride, as seen in Fig. 5b, a broad desorption peak is present in the range of 120 ~ 600 °C for the catalysts 1Au–xCeO_2/AC (x = 1, 3, 5, or 10), suggesting the existence of multi-state adsorption of hydrogen chloride. The desorption areas of hydrogen chloride for the catalysts 1Au–xCeO_2/AC (x = 1, 3, 5, or 10) are also larger than that of the Au/AC catalyst. The desorption area of hydrogen chloride gradually increases with the amount of CeO_2 additive. This demonstrates that the addition of CeO_2 can enhance the adsorption of acetylene and hydrogen chloride on the gold catalyst. Combined with the catalytic performance of the catalysts 1Au–xCeO_2/AC (x = 1, 3, 5, or 10), it indicates that CeO_2 additive with a Ce/Au molar ratio of 5 can improve considerably the adsorption of hydrogen chloride and acetylene on the catalyst, and eventually exhibit much higher catalytic activity for acetylene hydrochlorination than that of Au/AC catalyst (Fig. 1, 2).

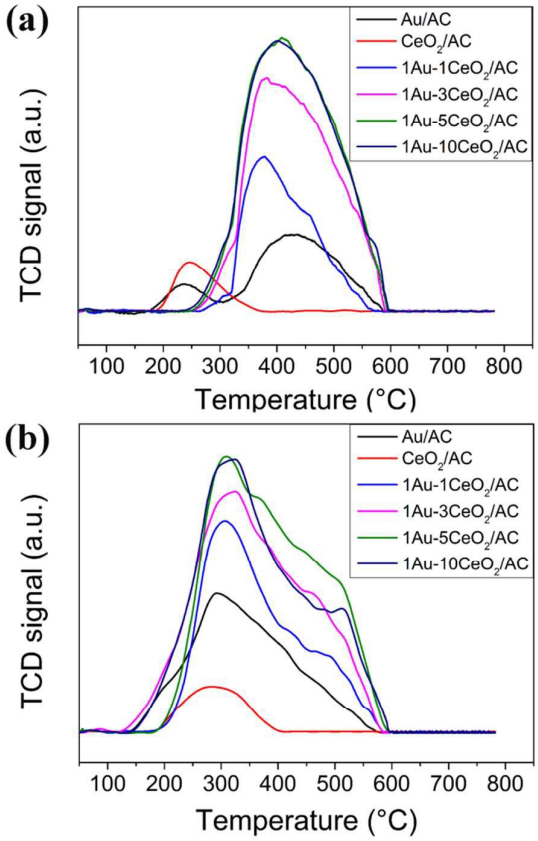

Fig. 5 (a) C_2H_2- and (b) HCl-TPD profiles of the fresh Au–CeO_2/AC catalysts.

3.2.4 Effect of CeO_2 additive on the valence of active species during the reaction

Fig. 6 shows the representative XRD patterns of AC, CeO_2, and the fresh and used Au-based catalysts. Apart from the amorphous diffraction peaks of AC (JCPDS 75–1621), no Au diffraction peak can be observed in the fresh catalyst Au/AC, suggesting gold nanoparticles below 4 nm or a material with a large amount of Au^{3+} centers.[11,35] In comparison, the used Au/AC distinctly shows typical diffraction peaks at 38.04^0, 44.16^0, 64.54^0 and 77.74^0, which can be assigned to the (111), (200), (220), and (311) planes of face-centered cubic (fcc) metallic Au^0 (JCPDS 04–0784), indicating the

reduction from Au^{3+} into Au^0 during the reaction. The crystallite size of the Au nanoparticles is about 12 nm for the used Au/AC, calculated by the Scherrer equation using the Au(111) diffraction peak, while the fresh 1Au/AC shows a size less than 4 nm, as listed in Table S2. As for the fresh and used 1Au–5CeO_2/AC, besides the amorphous diffraction peaks of AC and a typical cubic fluorite structure of CeO_2 (JCPDS 43–1002), no Au reflection peak is detected, in particular, the crystallite size of Au nanoparticles is less than 4 nm for both fresh and used 1Au–5CeO_2/AC. It is confirmed that the addition of CeO_2 can greatly inhibit the reduction of Au^{3+} into Au^0 during the reaction.

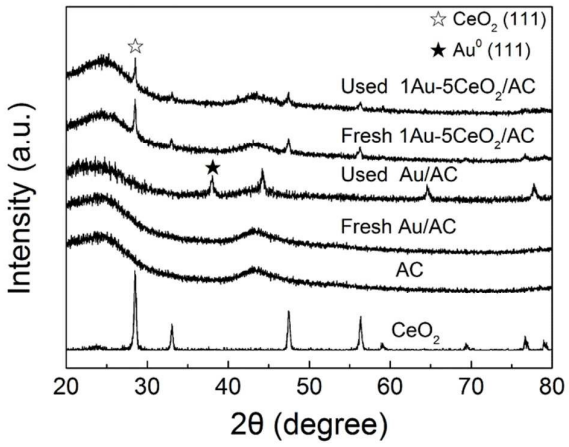

Fig. 6 Typical XRD patterns of the support AC, CeO_2, Au/AC, and 1Au–5CeO_2/AC catalyst.

XPS analysis was performed to determine the valence state and relative content of gold species in the catalysts Au/AC and 1Au–5CeO_2/AC before and after reaction. Fig. S4 displays the typical XPS spectra of the fresh catalysts Au/AC and 1Au–5CeO_2/AC, which distinctly demonstrates the signals of Au 4f and Ce 3d in the fresh catalyst

1Au–5CeO_2/AC. Fig. S5 shows the typical high-resolution XPS spectra of Au 4f for the catalysts Au/AC and 1Au–5CeO_2/AC before and after reaction. It is remarkable that more than one Au species exist, and the curve fitting is used to determine the relative content of each gold species[3]. As listed in Table 3, for all samples, there are three kinds of Au species, involving Au^{3+}, small metallic gold clusters of Au^0-s, and metallic Au^0.[3,36,37] The relative content of active component Au^{3+} in the fresh catalysts Au/AC and 1Au–5CeO_2/AC is 21.1% and 27.6%, respectively. The binding energy and relative content of gold species in different catalysts are listed in Table 3, the presence of CeO_2 additive makes the binding energy of Au^{3+} reduced by 0.2 eV, while that of Au^0 increased by 0.2 eV, comparing with those of the fresh catalyst Au/AC. It is illustrated that there is a strong interaction between Au and cerium species. Thus, electron transfers indeed occur between gold species and CeO_2 additive, leading to an increase of electron density around the Au^{3+} center but a decrease of electron density around the metallic Au^0 species, and then promoting the adsorption of hydrogen chloride and acetylene on the catalyst,[11,16,38,39] which is consistent with TPD results (Fig. 5). Comparing the content of Au^{3+} for the fresh and used catalysts, the content of Au^{3+} in the used Au/AC decreases from 21.1% to 12.1% whereas Au^0 increases from 54.3% to 66.4%, however, over the used 1Au–5CeO_2/AC the content of Au^{3+} only decreases from 27.6% to 25.1%. This indicates that CeO_2 additive can partially inhibit the reduction of active component Au^{3+} into metallic Au^0 during the catalyst preparation and the acetylene hydrochlorination reaction. Therefore, the strong interaction between gold and CeO_2 additive can suppress the reduction of active

species Au^{3+} into Au^{0} and enhance the catalytic activity for acetylene hydrochlorination.

Table 3 The relative content and binding energy of Au species in fresh and used catalysts, determined from the deconvolution of Au 4f XPS spectra.

Catalyst	Au species (Area %)			Binding energies (eV)		
	Au^{3+}	Au^{0}-s	Au^{0}	Au^{3+}	Au^{0}-s	Au^{0}
Fresh Au/AC	21.1	24.6	54.3	86.4	84.9	83.9
Used Au/AC	12.1	21.5	66.4	86.4	85.0	84.0
Fresh 1Au–5CeO_2/AC	27.6	25.9	46.5	86.2	84.9	84.1
Used 1Au–5CeO_2/AC	25.1	26.5	48.4	86.2	84.9	84.1

4 Conclusion

Gold–cerium oxide catalysts with different Ce/Au molar ratio were prepared using activated carbon as the support and cerium oxide as an additive, to study the effects of the addition of cerium oxide on the catalytic performance of Au-based catalysts for acetylene hydrochlorination. The optimal catalytic performance is obtained over 1Au–5CeO_2/AC catalyst with the acetylene conversion of 98.4% and the selectivity to VCM of 99.9% after 20 h on stream under the conditions of 180 °C and GHSV (C_2H_2) of 852 h^{-1}. Characterized through BET, AAS, TGA, TEM, Raman, XRD, TPR, TPD, and XPS, it is illustrated that the addition of cerium oxide can make active Au species

dispersed uniformly and improve the adsorption property of reactants on the catalysts, but also suppress the reduction of active gold species and inhibit the coking deposition on the catalyst surfaces during the reaction, eventually enhancing the activity and stability of the catalyst.

Acknowledgments

This work was supported by the Special Funds for the Major State Research Program of China (No. 2012CB720302) and the National Natural Science Foundation of China (21176174).

Reference

1 J. Zhang, N. Liu, W. Li and B. Dai, *Front. Chem. Sci. Eng.,* 2011, **5,** 514.
2 K. Zhou, J. Jia, C. Li, H. Xu, J. Zhou, G. Luo and F. Wei, *Green Chem.,* 2015, **17**, 356.
3 M. Conte, C. J. Davies, D. J. Morgan, T. E. Davies, A. F. Carley, P. Johnston and G. J. Hutchings, *Catal. Sci. Technol.*, 2013, **3**, 128.
4 M. Conte, C. J. Davies, D. J. Morgan, A. F. Carley, P. Johnston and G. J. Hutchings, *Catal. Lett.,* 2014, **144**, 1.
5 G. J. Hutchings, *J. Catal.,* 1985, **96**, 292.
6 M. Conte, A. F. Carley, C. Heirene, D. J. Willock, P. Johnston, A. A. Herzing, C. J. Kiely and G. J. Hutchings, *J. Catal.,* 2007, **250**, 231.
7 M. Conte, A. F. Carley, G. Attard, A. A. Herzing, C. J. Kiely and G. J. Hutchings, *J. Catal.,* 2008, **257**, 190.
8 M. Conte, A. F. Carley and G. J. Hutchings, *Catal. Lett.,* 2008, **124**, 165.
9 J. Zhao, T. Zhang, X. Di, J. Xu, S. Gu, Q. Zhang, J. Ni and X. Li, *Catal. Sci. Technol.,* 2015, in press.
10 B. Nkosi, M. D. Adams, N. J. Coville and G. J. Hutchings, *J. Catal.,* 1991, **128**, 378.
11 H. Zhang, W. Li, X. Li, W. Zhao, J. Gu, X. Qi, Y. Dong, B. Dai and J. Zhang, *Catal. Sci. Technol.,* 2015, **5**, 1870.
12 J. Zhao, J. Xu, J. Xu, J. Ni, T. Zhang, X. Xu and X. Li, *ChemPlusChem,* 2015, **80**, 196.
13 K. Zhou, W. Wang, Z. Zhao, G. Luo, J. T. Miller, M. S. Wong and F. Wei, *ACS Catal.,* 2014, **4**, 3112.
14 H. Zhang, B. Dai, W. Li, X. Wang, J. Zhang, M. Zhu and J. Gu, *J. Catal.,* 2014, **316**, 141.

15 Y. Pu, J. Zhang, X. Wang, H. Zhang, L. Yu, Y. Dong and W. Li, *Catal. Sci. Technol.,* 2014, **4**, 4426.
16 C. Huang, M. Zhu, L. Kang, X. Li and B. Dai, *Chem. Eng. J.,* 2014, **242**, 69.
17 S. Wang, B. Shen and Q. Song, *Catal. Lett.,* 2010, **134**, 102.
18 H. Zhang, B. Dai, W. Li, X. Wang, J. Zhang, M. Zhu and J. Gu, *J. Catal.,* 2014, **316**, 141.
19 X. S. Huang, H. Sun, L. C. Wang, Y. M. Liu, K. N. Fan and Y. Cao, *Appl. Catal., B,* 2009, **90**, 224.
20 K. Qian, S. Lv, X. Xiao, H. Sun, J. Lu, M. Luo and W. Huang, *J. Mol. Catal. A: Chem.,* 2009, **306**, 40.
21 Y. Jiao, F. Wang, X. Ma, Q. Tang, K. Wang, Y. Guo and L. Yang, *Microporous Mesoporous Mater.,* 2013, **176**, 1.
22 S. Zhang, X. S. Li, B. Chen, X. Zhu, C. Shi and A. M. Zhu, *ACS Catal.,* 2014, **4**, 3481.
23 Q. Fu, A. Weber and M. Flytzani-Stephanopoulos, *Catal. Lett.,* 2001, **77**, 87.
24 R. Si and M. Flytzani-Stephanopoulos, *Angew. Chem.,* 2008, **120**, 2926.
25 H. F. Li, N. Zhang, P. Chen, M. F. Luo and J. Q. Lu, *Appl. Catal., B,* 2011, **110**, 279.
26 H. Y. Kim, H. M. Lee and G. Henkelman, *J. Am. Chem. Soc.,* 2011, **134**, 1560.
27 B. Nkosi, N. J. Coville and G. J. Hutchings, , *J. Chem. Soc., Chem. Commun.,* 1988, **1**,71.
28 Q. L. Song, S. J. Wang, B. X. Shen and J. G. Zhao, *Pet. Sci. Technol.,* 2010, **28**, 1825.
29 B. Nkosi, N. J. Coville, G. J. Hutchings, M. D. Adams, J. Friedl, and F. E. Wagner, *J. Catal.,* 1991, **128**, 366.
30 M. Gurrath, T. Kuretzky, H. P. Boehm, L. B. Okhlopkova, A. S. Lisitsyn and V. A. Likholobov, *Carbon,* 2000, **38**, 1241.
31 J. K. Brennan, T. J. Bandosz, K. T. Thomson and K. E. Gubbins, *Colloids Surf., A,* 2001, **187–188**, 539.
32 S. R. de Miguel, O. A. Scelza, M. C. Román-Martínez, C. Salinas-Martínez de Lecea, D. Cazorla-Amorós and A. Linares-Solano, *Appl. Catal., A,* 1998, **170**, 93.
33 K. Dumbuya, G. Cabailh, R. Lazzari, J. Jupille, L. Ringel, M. Pistor, O. Lytken, H. P. Steinrück and J. M. Gottfried, *Catal. Today,* 2012, **181**, 20.
34 J. C. Serrano-Ruiz, E. V. Ramos-Fernández, J. Silvestre-Albero, A. Sepúlveda-Escribano and F. Rodríguez-Reinoso, *Mater. Res. Bull.,* 2008, **43**, 1850.
35 M. Conte, C. J. Davies, D. J. Morgan, T. E. Davies, D. J. Elias, A. F. Carley, P. Johnston and G. J. Hutchings, *J. Catal.,* 2013, **297**, 128.
36 C. N. R. Rao, V. Vijayakrishnan, H. N. Aiyer, G. U. Kulkarni and G. N. Subbanna, *J. Phys. Chem.,* 1993, **97**, 11157.
37 T. V. Choudhary and D. W. Goodman, *Top. Catal.,* 2002, **21**, 25.
38 J. Zhang, Z. He, W. Li and Y. Han, *RSC Adv.,* 2012, **2**, 4814.
39 B. Wang, L. Yu, J. Zhang, Y. Pu, H. Zhang and W. Li, *RSC Adv.,* 2014, **4**, 15877.

Graphical Abstract